

Interstitial Fluid Pressurization During Confined Compression Cyclical Loading of Articular Cartilage

MICHAEL A. SOLTZ and GERARD A. ATESHIAN

Department of Mechanical Engineering, Columbia University, New York, NY

(Received 17 September 1998; accepted 21 October 1999)

Abstract—The objective of this study was to experimentally verify the well-accepted but untested hypothesis that cartilage interstitial fluid pressurizes variously under the action of an applied cyclical stress in confined compression over a range of loading frequencies, contributing significantly to the cartilage dynamic stiffness. Eighteen bovine cartilage cylindrical samples were tested under load control using a porous indenter in a confined compression chamber fitted with a microchip pressure transducer at its bottom. Over a static stress of 130 kPa, a cyclical stress of amplitude 33 kPa was applied with the indenter at frequencies ranging from 0.0001 to 0.1 Hz. The cartilage interstitial fluid pressure and deformation were measured simultaneously as a function of time. The displacement response at the lowest tested frequency was curvefitted in the time domain to determine the linear biphasic material properties, $H_A = 0.70 \pm 0.10$ MPa and $k_0 = 2.4 \times 10^{-16} \pm 0.64 \times 10^{-16}$ m⁴/N s. These properties were employed in the biphasic theory to predict the interstitial fluid pressure response and compare it to experiment, resulting in nonlinear coefficients of determination ranging from $r^2 = 0.89 \pm 0.15$ to 0.96 ± 0.03 depending on frequency. It was found for the samples of this study that above a characteristic frequency of 0.00044 Hz, the magnitude and phase of fluid pressurization matched the applied stress, reducing the tissue strain at the impermeable bottom surface to nearly zero. The findings of this study verify the hypothesis that cartilage dynamic stiffness derives primarily from flow-dependent viscoelasticity as predicted by the linear biphasic theory; they demonstrate experimentally the significance of interstitial fluid pressurization as the fundamental mechanism of cartilage load support over a wide range of frequencies.
© 2000 Biomedical Engineering Society.
[S0090-6964(00)00202-2]

Keywords—Biphasic theory, Diarthrodial joints, Cartilage stresses.

INTRODUCTION

Articular cartilage is a hydrated soft tissue which serves as the bearing material of diarthrodial joints. The mechanical response of cartilage has been investigated in many studies and it is generally accepted that its vis-

coelastic response is primarily contributed by the resistive drag of interstitial fluid flowing through the low-permeability collagen-proteoglycan matrix. Porous media models have been proposed which describe this mechanical response under various loading conditions^{11,27} and it has been demonstrated from these theories that the dynamic stiffening of cartilage under cyclical loading at various frequencies could be explained by the pressurization of interstitial water which thus contributes to the load support across the tissue.^{11,21} Interestingly however, there have been no experimental verifications of this well-accepted dynamic interstitial fluid pressurization mechanism. Furthermore, some studies have suggested that intrinsic viscoelasticity of the cartilage solid matrix may also contribute significantly to the dynamic response of cartilage,^{23,32} raising a question as to the relative importance of flow-dependent and flow-independent viscoelasticity in articular cartilage.

Understanding the role of interstitial fluid pressurization in the mechanical response of articular cartilage is of great interest to various investigators. Theoretical porous media analyses^{2,19,22} have demonstrated that fluid pressurization contributes to supporting upwards of 90% of the applied stress during contact of cartilage layers. Recently, direct experimental measurements of interstitial fluid pressurization during confined compression creep and stress relaxation^{28,33} have indeed confirmed that upward of 90% of the total applied stress can be supported by the interstitial fluid pressure for several hundred seconds after loading. This suggests that for *in vivo* loading situations where contact tractions can be typically as high as 12 MPa, the fluid pressure could act to shield the solid matrix of collagen by maintaining the effective collagen matrix stress at the level of, e.g., 1.2 MPa only. The implications of this mechanism are significant not only in the understanding of cartilage mechanics and tribology^{1,3,22,25,37} but also cartilage biology, since many studies explore the biosynthesis of live cartilage explants under various loading conditions. Therefore, it is important to verify experimentally under what

Address correspondence to Dr. Gerard A. Ateshian, Department of Mechanical Engineering, Columbia University, 500 W. 120th St., Rm. 220 Mudd Bldg., New York, NY 10027. Electronic mail: ateshian@columbia.edu

loading conditions the interstitial fluid of cartilage pressurizes.

Since activities of daily living such as walking and running typically involve cyclical loading, many researchers have been interested in different aspects of the tissue response to sinusoidal loading from the cellular to the continuum level. Investigators have demonstrated various cellular responses due to different loading stimuli by applying either a cyclical load³⁶ or displacement,^{7,9,13,29,30} at varying frequencies and amplitudes, thereby observing biosynthetic responses in the chondrocyte cell. Often, these responses have been associated with only the applied strain or total stress, however, the influence of fluid pressure in those specific loading configurations was not directly assessed. While the correlation of biosynthetic response to fluid pressure is not the focus of the present study, elucidating the mechanical environment of chondrocytes would be beneficial and add to the interpretation of established findings. The mechanical response of cartilage to cyclical loading has also been studied both theoretically^{11,16,21,33,34,35} and experimentally.^{8,10,11,17,21,30,36} However, the extent and significance of interstitial fluid pressurization under cyclical loading remains to be directly demonstrated. Therefore, the objective of this study is to verify experimentally the hypothesis that interstitial fluid pressurizes variously at different loading frequencies under the action of an applied cyclical stress in confined compression, and that this pressurization can be predicted by the linear biphasic theory for soft hydrated tissues²⁶ which incorporates only flow-dependent viscoelasticity. The methodology employed for measuring interstitial fluid pressure at the articular surface is based on our earlier study³³ and is conceptually similar to that of Oloyede and Broom.²⁸

MATERIALS AND METHODS

Healthy calf (2–4 month) carpometacarpal joints were obtained from a local abattoir and stored for 4–5 h at 4 °C until preparation. The joint capsule was then dissected to expose the cartilage surfaces and a circular punch (diam=6.75 mm) was pressed perpendicularly onto the cartilage surface to core out cartilage-bone plugs. Each plug was placed on a freezing stage (Hacker Instruments, Fairfield, NJ) mounted on a sledge microtome (model 1400; Leitz, Rockleigh, NJ) with the articular surface face down and parallel to the blade. The full-thickness plug was microtomed to remove residual subchondral bone and vascularized deep zone only, leaving the articular surface intact. The thickness of the plug was measured using a custom micrometer thickness measurement device at three different locations on the surface to provide an average thickness measurement for the specimen (the measurement variability over the three lo-

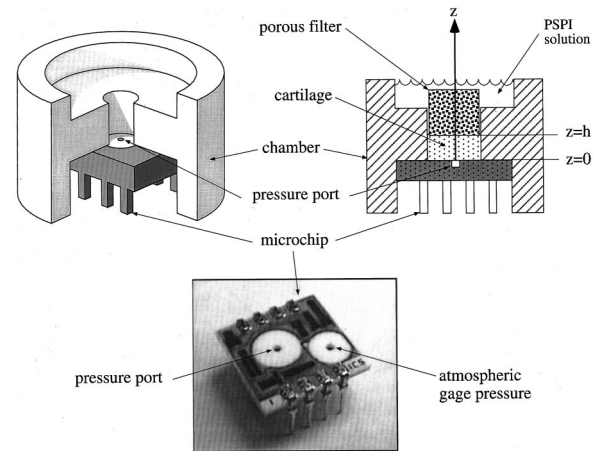


FIGURE 1. Schematic of confined compression chamber with microchip pressure transducer.

cations averaged 0.05 mm). During the preparation process, the specimens were kept moist in buffered physiologic saline containing protease inhibitors (PSPI: 2 mM ethylenediamine tetra-acetate acid, 5 mM benzamide, 10 mM *N*-ethylmaleimide, 1 mM phenylmethyl-sulfonyl fluoride, 0.15 M NaCl). The specimens were stored at –80 °C until ready for use, at which time they were thawed and allowed to equilibrate in PSPI solution for 1 h.

The confined compression chamber (diam=6.53 mm) employed for this study incorporated a solid-state piezoresistive microchip pressure transducer (NPC 1210-050G-3N; Lucas NovaSensor, Fremont, CA; range 0–345 kPa gauge pressure; $\pm 0.1\%$ accuracy; linearity of 0.1% of full-scale output; pressure port 1 mm diam \times 1 mm deep; frequency response >1 kHz) bonded to the bottom of the chamber (Fig. 1) as reported previously.³³ Each cartilage plug was placed with its articular surface side facing the fluid-filled pressure port of the microchip transducer in order to measure the cartilage interstitial fluid pressure at the center of that surface. Both the side wall and bottom surface of the chamber were impermeable. Because of the slight mismatch between the chamber and specimen diameters, the cartilage plug fit snugly within the chamber with no clearance along the side wall. Loading of the top surface of the specimen was performed with a free-draining porous indenter (diam=6.30 mm, 50% porosity, 45–53 μ m pore size, permeability four orders of magnitude greater than cartilage), immersed entirely in the surrounding PSPI bath to prevent capillary uplift effects.

Eighteen specimens were tested under load control to determine the tissue response to an applied cyclical stress using a testing apparatus described previously,¹⁴ and the confined compression testing chamber (Fig. 1). A data acquisition and control program was created using

Labtech Notebook (Laboratory Technologies Corporation, Wilmington, MA) which employed a feedback loop to compare a desired sinusoidal load to the actual applied load, measured by a load cell (Sensotec, model 31, Columbus, OH, range ± 45 N). Depending on whether the load was greater or less than the desired signal the program would actuate up or down a computer-controlled stepper micrometer (Oriel Corp., model 18515, Stratford, CT) connected to the porous indenter. The actual indenter displacement was measured with a linear variable differential transformer (LVDT) (Schaevitz, model HR100, Hampton, VA). Initially, a tare load of 4.5 N (130 kPa) was applied to ensure proper seating of the specimen in the chamber; this tare load was maintained for the entire duration of the experiment. From previous experience^{4,33} it has been observed that such relatively elevated tare loads are required to provide sufficient lateral confinement of the tissue and to prevent the appearance of an initial jump in the surface displacement under an applied load;²⁷ an initial jump would otherwise be indicative of a lateral tissue expansion that would violate the intended premise of a one-dimensional testing configuration. Because it was possible to monitor the interstitial fluid pressure at the interface with the pressure port, the cyclical test was not initiated until the pressure resulting from the application of the tare load returned to nearly zero, indicating near-equilibrium conditions. Since the protocol of this study called for long testing durations (up to $\sim 30,000$ s), near-equilibrium tare conditions were assumed when the fluid pressure dropped below a threshold value of approximately 1.4 kPa ($\ll 130$ kPa) to minimize the tissue degradation that might occur as a result of the testing duration. In the theoretical analysis, it was thus necessary to provide a small adjustment to account for the fact that the tissue had not fully reached equilibrium at the initiation of sinusoidal loading, as described below. Frequencies ranging from 0.0001 to 0.1 Hz for one batch of specimens (group I), and from 0.0005 to 0.05 Hz for another batch (group II) were tested at decade intervals (e.g., 0.0001, 0.001, etc.) with an applied load amplitude of 1 N (total stress amplitude of 33 kPa); thus, the total load applied to the specimen consisted of the tare load superposed with the sinusoidal load. During these tests, the displacement at the cartilage-porous indenter interface ($z=h$) was measured with the LVDT, while simultaneously measuring the fluid pressure at the interface of the articular surface and pressure port ($z=0$). Compliance of the entire system was quantified prior to testing of the cartilage specimens by determining the load-displacement response of the apparatus in the absence of a test sample (i.e., with the porous filter directly contacting the bottom of the test chamber). The resulting compliance curve, which was found to be linear with a slope of $2.85 \mu\text{m/N}$, was subsequently used to properly subtract the load-

dependent deformation due to system compliance from the LVDT measurements of cartilage deformation.

To compare experimental results with theory, a curve-fitting program based on the linear biphasic theory²⁷ was first employed to determine the material parameters of the tissue. The biphasic theory models cartilage as a mixture of an intrinsically incompressible solid phase representing the collagen-proteoglycan-chondrocyte matrix and an intrinsically incompressible fluid phase representing interstitial water. Overall tissue compressibility results from fluid transport into or out of the porous-permeable solid matrix. The dissipative drag exerted by the fluid flowing relative to the low-permeability solid matrix imparts a viscoelastic response to the tissue. The general equations of the biphasic theory can be found elsewhere;²⁷ the reduction of those general equations for the configuration of confined compression has also been described previously^{11,21,27,35} and is summarized below. The governing equation for confined compression of a linear isotropic homogeneous biphasic material is given by

$$\frac{\partial^2 u}{\partial z^2} - \frac{1}{H_A k_0} \frac{\partial u}{\partial t} = 0, \quad (1)$$

where $u(z,t)$ is the displacement of the solid phase, H_A is the aggregate modulus, and k_0 is the permeability of the tissue (assumed constant in the linear biphasic theory). The initial condition at $t=0$ is

$$u(z,0) = 0, \quad (2)$$

and the boundary condition at the bottom, impermeable interface ($z=0$, Fig. 1) is

$$u(0,t) = 0.$$

For sinusoidal loading at the cartilage-porous indenter interface ($z=h$), the boundary condition is

$$H_A \left. \frac{\partial u}{\partial z} \right|_{z=h} = -P_A \sin 2\pi f t - P_0, \quad (3)$$

where $P_A \sin 2\pi f t$ is the applied total compressive stress of amplitude P_A and frequency f , and P_0 is a small superimposed static compressive stress ($P_0 \ll P_A$) whose value is adjusted to account for near-equilibrium experimental conditions at the completion of tare loading, prior to the initiation of sinusoidal loading, as described above. The boundary condition of Eq. (3) derives from the fact that the total stress at any z is given by $\sigma(z,t) = -p(z,t) + H_A \partial u / \partial z$; however, at the free-draining porous interface, $p(h,t) = 0$. Note also that $\sigma(z,t)$ is uni-

form through the depth because of momentum conservation, i.e., $\sigma(z,t) \equiv \sigma(t)$, which can be used to evaluate $p(z,t)$ at any z . Solving Eq. (1) subject to Eqs. (2) and (3) yields^{27,35}

$$\begin{aligned} \frac{u(z,t)}{h} = & -\frac{P_0}{H_A} \left[\frac{z}{h} - 2 \sum_{n=1}^{\infty} \frac{(-1)^{n-1}}{\alpha_n^2} \sin\left(\alpha_n \frac{z}{h}\right) \right. \\ & \left. \times \exp\left(-\alpha_n^2 \frac{H_A k_0}{h^2} t\right) \right] \\ & - 2 \frac{P_A}{H_A} \sum_{n=1}^{\infty} \frac{(-1)^{n-1}}{\left(\frac{2\pi f h^2}{H_A k_0}\right)^2 + \alpha_n^4} \sin\left(\alpha_n \frac{z}{h}\right) \\ & \times \left(\alpha_n^2 \sin 2\pi f t - \frac{2\pi f h^2}{H_A k_0} \cos 2\pi f t \right. \\ & \left. + \frac{2\pi f h^2}{H_A k_0} \exp\left(-\alpha_n^2 \frac{H_A k_0}{h^2} t\right) \right), \end{aligned} \quad (4)$$

where $\alpha_n = (n - \frac{1}{2})\pi$. The time-dependent experimental displacement curve can be least squares fitted with the theoretical biphasic solution of Eq. (4), evaluated at $z = h$, to determine the specimen-specific material parameters H_A and k_0 from the sinusoidal experiment conducted at the lowest frequency (i.e., 0.0001 Hz for group I and 0.0005 Hz for group II). However, in practice, it is computationally more efficient to solve the partial differential equation of Eq. (1), subject to the boundary conditions of Eqs. (2) and (3), using a numerical finite difference scheme, as done in this study, with the analytical solution of Eq. (4) serving as a verification of the numerical scheme. An added advantage of this approach is that the ideal boundary condition for the applied sinusoidal load [in Eq. (3) above] can further be substituted with the actual applied load (as measured during the experiment), which may deviate slightly from the desired ideal sinusoidal function due to the testing apparatus' controller and system dynamics (the deviation from an ideal sinusoidal function was assessed using the total harmonic distortion²¹). The quality of these curvefits was assessed using the coefficient of determination r^2 defined by the expression²⁰

$$r^2 = 1 - \frac{\sum (y - y_{\text{est}})^2}{\sum (y - \bar{y})^2}, \quad (5)$$

where y represents the observed (experimental) variable, y_{est} is the estimated (theoretical) variable, \bar{y} is the mean value of y , and summations are taken over all observations (all sampled time steps). Once the parameters H_A and k_0 were determined from curvefitting the surface displacement at the lowest frequency, they were em-

ployed in the theory to predict the measured surface displacement at all higher frequencies using Eq. (4), and to predict the measured interstitial fluid pressure at all frequencies, at the impermeable interface $z=0$, given by

$$p(0,t) = H_A \left(\frac{\partial u}{\partial z} \Big|_{z=0} - \frac{\partial u}{\partial z} \Big|_{z=h} \right), \quad (6)$$

where the expression for u can be taken from Eq. (4) although in practice its numerical solution is employed instead. The quality of these predictions was similarly assessed against experimental measurements using the generalized nonlinear correlation coefficient of Eq. (5).

The amplitude of the measured displacement and fluid pressure and the phase angle with respect to the applied cyclical stress were determined at each frequency using fast Fourier transforms.

RESULTS

Eighteen specimens were tested in total ($h=0.62 \pm 0.08$ mm, after tare loading); the nine specimens of group I were each tested for N cycles (see below) at the loading frequencies $f=0.1$ Hz ($N=4$ cycles), 0.01 Hz ($N=4$ cycles), 0.001 Hz ($N=4$ cycles), 0.0001 Hz ($N=2$ cycles) and the nine specimens of group II were each tested at $f=0.05$ Hz ($N=4$ cycles), 0.005 Hz ($N=4$ cycles), and 0.0005 Hz ($N=3$ cycles). At the completion of cyclical loading at each frequency, the specimen was allowed to recover prior to initiating loading at the next lower frequency. For all tests, P_A was set to 33 kPa; the total harmonic distortion in the sinusoidal profile of the applied cyclical stress ranged from an average of 1.8% at 0.0001 Hz to 10.6% at 0.1 Hz. The total duration of testing, including tare loading, cyclical loading and recovery time, averaged 30,000 s for group I specimens tested in the range of 0.0001–0.1 Hz and 13,000 s for group II specimens tested in the range of 0.0005–0.05 Hz. In the presentation of figures which follows, all displacement and pressure results are reported relative to the tare configuration where the tissue sample is under an equilibrium compressive total stress of 130 kPa and near-zero interstitial fluid pressure. The average value of the adjusted offset parameter P_0 needed to account for near-equilibrium conditions was 2.0 ± 2.6 kPa. A typical curvefit for the displacement $u(h,t)$ at 0.0001 Hz is shown in Fig. 2(a); curvefitting of all nine specimens of group I at this frequency was achieved with $r^2=0.98 \pm 0.04$. Curvefitting of the nine specimens of group II at 0.0005 Hz yielded $r^2=0.94 \pm 0.05$. The material properties determined from curvefitting the lowest frequency displacement of all 18 specimens were $H_A=0.70 \pm 0.10$ MPa and $k_0=2.4 \times 10^{-16} \pm 0.64 \times 10^{-16}$ m⁴/N s. Comparison of experimental and predicted fluid

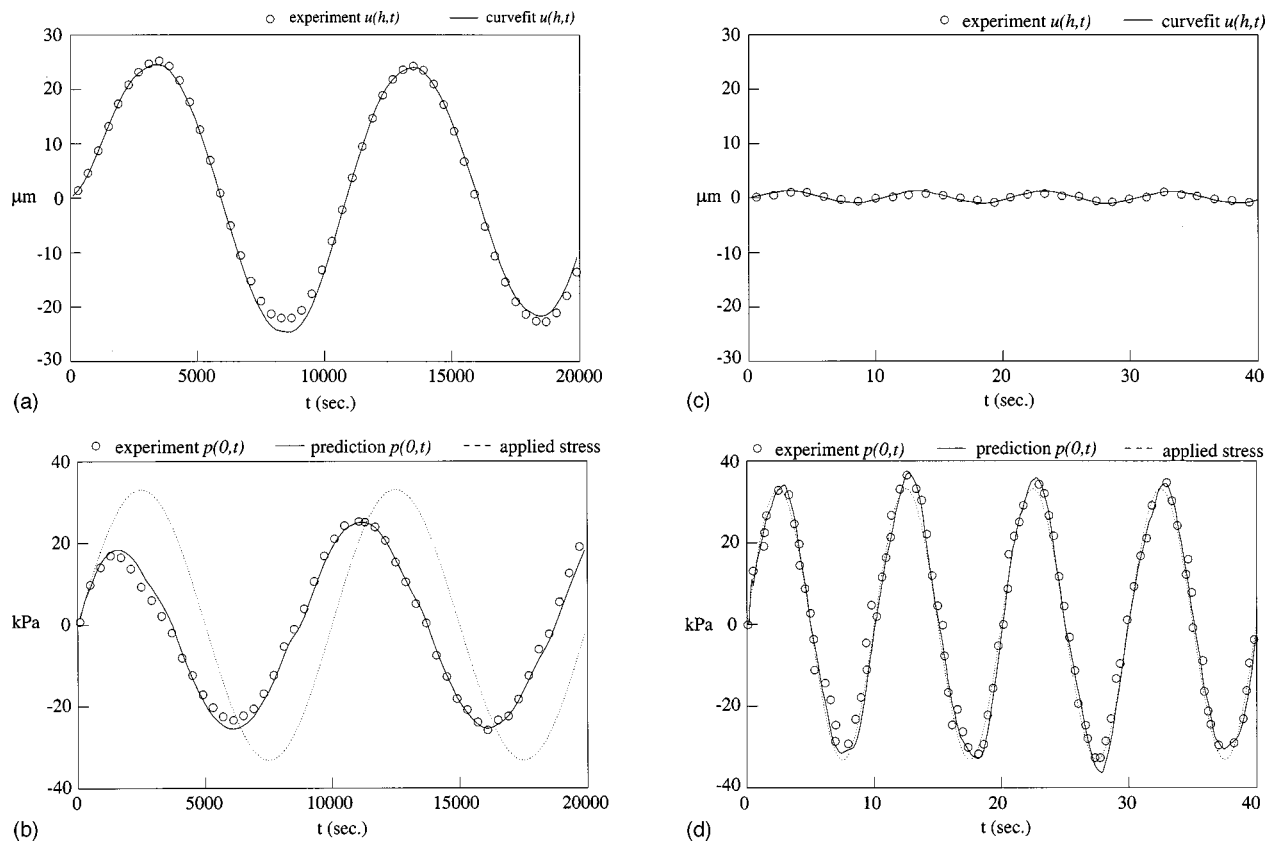


FIGURE 2. (a) Curvefit of 0.0001 Hz displacement and experimental data for typical specimen. (b) Prediction of 0.0001 Hz fluid pressure and experimental data for same specimen. (c) Prediction of 0.1 Hz displacement and experimental data for same specimen. (d) Prediction of 0.1 Hz fluid pressure and experimental data for same specimen.

pressure, $p(0,t)$, produced $r^2 = 0.90 \pm 0.10$ at 0.0001 Hz [Fig. 2(b), displayed with total stress $\sigma(t)$] and $r^2 = 0.94 \pm 0.05$ at 0.0005 Hz. An example of prediction of displacement and pressure for the highest frequencies is shown in Figs. 2(c) and 2(d), respectively. Correlations between experimental data and theoretical predictions for all frequencies are summarized in Table 1. The amplitude of the displacement and pressure responses over the entire frequency range, averaged over all specimens, are shown in Figs. 3(a) and 3(c), respectively, together with the corresponding theoretical frequency response gener-

ated from the steady-state response of Eq. (4) (see the Appendix) using the average value for the aggregate modulus²⁷ and permeability. Also of interest are the corresponding phase angle diagrams for the displacement and pressure, shown in Figs. 3(b) and 3(d), respectively.

DISCUSSION

The objective of this study was to experimentally verify the well-accepted but untested hypothesis that cartilage interstitial fluid pressurizes under dynamic loading, thus contributing significantly to the dynamic stiffening and flow-dependent viscoelasticity of this tissue. The experimental results of this study demonstrated unequivocally that such pressurization does take place with increasing loading frequency [Figs. 2(b) and 3(c)], concurrently with a decrease in tissue compliance [Figs. 2(a), 2(c), and 3(a)]; conclusive agreement was also found between the linear biphasic theory and experiments as indicated by the ability not only to curvefit displacements at low frequencies but also to predict fluid pressure at all frequencies and displacements at the frequencies other than that used for curvefitting (Table 1 and Figs. 2 and 3). Therefore, it is reasonable to explain

TABLE 1. Summary of the correlation coefficients for predicted displacements and fluid pressure at various frequencies.

Frequency (Hz)	r^2 displacement	r^2 fluid pressure
0.0001	...	0.90 ± 0.10
0.0005	...	0.96 ± 0.03
0.001	0.96 ± 0.03	0.91 ± 0.05
0.005	0.78 ± 0.13	0.95 ± 0.02
0.01	0.90 ± 0.04	0.91 ± 0.05
0.05	0.73 ± 0.11	0.93 ± 0.05
0.1	0.65 ± 0.19	0.89 ± 0.15

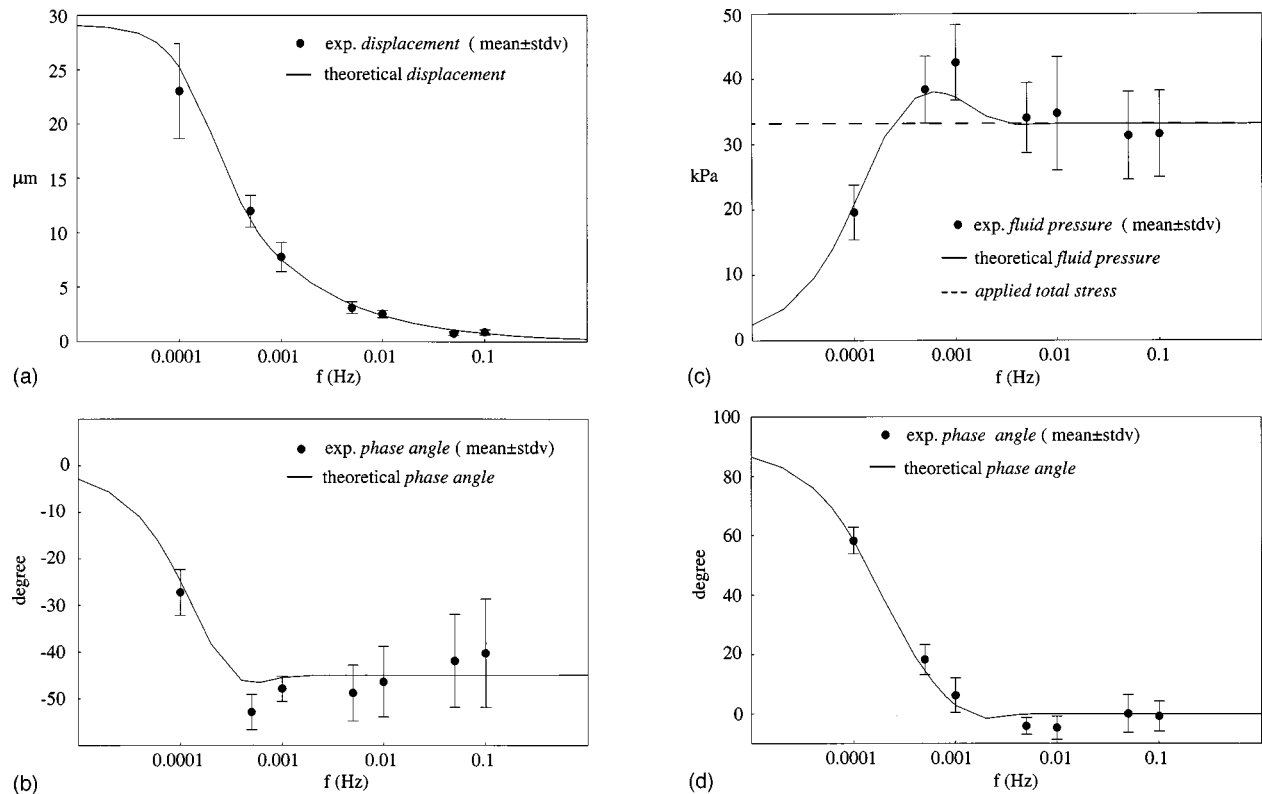


FIGURE 3. (a) Experimental and theoretical displacement magnitude for all specimens over the frequencies tested. (b) Experimental and theoretical phase shift of displacement relative to applied stress for all specimens over the frequencies tested. (c) Experimental and theoretical fluid pressure magnitude for all specimens over the frequencies tested. (d) Experimental and theoretical phase shift of fluid pressure relative to applied stress for all specimens over the frequencies tested.

the observed experimental phenomena on the basis of what is known from theory. Accordingly, the total stress in the tissue is a combination of the interstitial fluid pressure and elastic stress due to deformation and strain of the solid matrix ($\sigma = -p + H_A \partial u / \partial z$). The interaction between these stress components varies as a function of loading frequency (Fig. 3). According to the biphasic analysis of this confined compression problem,^{11,21,35} there exists a characteristic frequency which marks the transition between two regimes at opposite ends of the frequency spectrum; this characteristic frequency is given by $f_c = H_A k_0 / h^2$ (the inverse of the ‘‘gel time constant’’^{11,18,21,27}) which averages to 0.00044 Hz for the material properties and specimen thicknesses found in this study. For very low loading frequencies, $f \ll f_c$, the tissue rate of deformation is sufficiently slow that interstitial water has ample time to flow in and out of the specimen with negligible drag against the solid matrix. Consequently, the interstitial fluid pressurizes negligibly throughout the depth of the tissue, including at the pressure port interface [Fig. 3(c)], and the majority of the applied stress must be supported by the elastic stress in the solid matrix; the deformation of the cartilage plug is then greatest at those lower frequencies [Fig. 3(a),

$f < 0.0001$ Hz] and more in phase with the applied stress [Fig. 3(b), $f < 0.0001$ Hz]. Conversely, at high loading frequencies, $f \gg f_c$, the rate at which the load is applied greatly exceeds the rate at which the fluid can flow with negligible resistance through the porous-permeable matrix. Since fluid must nevertheless flow into and out of the tissue because of the requirement for conservation of mass, a large pressure gradient must build up inside the tissue to overcome the large drag force between the solid and fluid phases. This causes the pressure at the impermeable interface to rise substantially [Figs. 2(c) and 3(c), $f > 0.005$ Hz], coming into phase with the applied stress [Fig. 3(d)]. This rise in pressure supports the majority of the total applied stress through most of the depth of the tissue (except in a narrow region near the porous indenter), reducing the amount of elastic stress, strain, and deformation in the solid matrix [Figs. 2(a) and 3(a), $f > 0.005$ Hz]. Effectively, the amplitude of the fluid pressure approaches that of the total applied stress (33 kPa) when f is much greater than 0.00044 Hz [e.g., at 0.1 Hz in Fig. 2(d)], signifying that nearly 100% of the total stress outside of the narrow region near the porous indenter is supported by interstitial fluid pressurization

and that tissue strain is negligibly small where the fluid pressure is high. It should be understood that the solid collagen-proteoglycan matrix is still subjected to the hydrostatic pressure exerted by the surrounding interstitial fluid, which may have biological implications in relation to cartilage metabolism.^{13,15,29,30,36} However, this hydrostatic pressure does not cause measurable deformation of the cartilage extracellular matrix.⁶

At intermediate loading frequencies, $f \approx f_c$, the two opposite trends compete to produce non-negligible tissue deformation and interstitial fluid pressurization, as can be observed, for example, at $f = 0.0001$ Hz in Figs. 2(a) and 2(b). Interestingly, there exists a range of frequencies about f_c where the interstitial fluid pressure amplitude p exceeds that of the total applied stress σ . This can occur when the elastic strain at the pressure port interface is tensile (relative to the tare configuration) while the total stress is compressive (and vice versa), i.e., when the cyclical deformation most lags behind the total stress [Fig. 3(b)].

It is noteworthy that, the apparent tissue stiffness $G = \sigma/(u/h)$,^{8,11,21} increases with frequency, as can be construed from Fig. 3(a), and as previously reported by others;^{11,21} this can be explained by the increase in interstitial fluid pressure which supports greater load, as verified experimentally, producing a concomitant decrease in tissue deformation. In confined compression, as the tissue displacement amplitude approaches zero with increasing frequency [Fig. 3(a)], there is no upper limit to the increase in the apparent stiffness;¹¹ for example, at $f = 0.1$ Hz, $G \approx 20$ MPa yet the true solid matrix compressive tissue stiffness is 30 times smaller at $H_A = 0.70$ MPa.

The direct measurement of interstitial fluid pressure in this study firmly establishes that the viscoelastic response of cartilage is primarily contributed by the viscous drag of the interstitial fluid as it flows through the porous-permeable collagen-proteoglycan matrix, with the pressure gradient acting as the driving force. For the purpose of comparison, the effect of incorporating intrinsic solid matrix viscoelasticity in the theoretical analysis of dynamic confined compression is presented in Fig. 4, where the pressure and displacement amplitude responses are compared between the linear biphasic theory²⁷ and the linear biphasic poroviscoelastic²³ (BPVE) theory (see the Appendix for a presentation of the governing equations). The latter is a generalization of the former, modeling the solid matrix with the quasilinear viscoelasticity theory.¹² Typical viscoelasticity material constants are obtained from the literature.³² It can be observed from Fig. 4 that it is qualitatively easier to distinguish the responses of these two models from the pressure amplitudes, since the displacement amplitudes are less distinct for the given choice of material constants. This finding further supports the usefulness of experimental pressure measure-

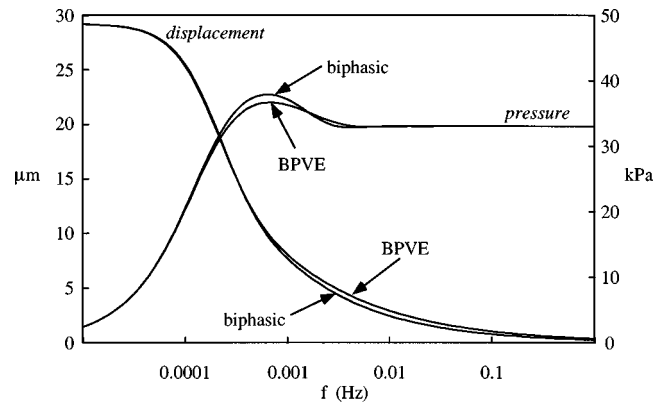


FIGURE 4. Displacement and pressure amplitude responses in confined compression cyclical loading as a function of loading frequency for the linear biphasic theory and the BPVE. Tissue thickness, cyclical load amplitude, and material properties for biphasic and BPVE models: $h = 0.62$ mm, $P_A = 33$ kPa, $H_A = 0.70$ MPa, $k_0 = 2.4 \times 10^{-16}$ m⁴/N s. Additional constants for BPVE (Ref. 32): $c = 0.16$, $\tau_1 = 0.06$ s, $\tau_2 = 201$ s (see the Appendix).

ments for assessing the relative role of flow-dependent and flow-independent viscoelasticity; by comparing the pressure amplitude responses from Fig. 4 with the experimental results of Fig. 3(c), it is observed that incorporating intrinsic solid matrix viscoelasticity into the analysis reduces the peak pressure amplitude and shifts it to the right, which results in a slightly greater deviation between theory and experiment. These results demonstrate that the incorporation of flow-independent viscoelasticity does not produce better agreement between theory and experiment in confined compression with cyclical loading, in the case of immature bovine cartilage. Based on preliminary calculations not presented here, it is speculated that improved agreement between theory and experiment is more likely to be achieved by incorporating the inhomogeneity of the material properties through the tissue depth,³¹ whereas the current analysis assumed homogeneous properties.

The results of this study emphasize the need to account for interstitial fluid pressurization when determining cartilage stiffness under dynamic conditions to avoid misleading interpretations of experimental results. They also clarify how cartilage, with a compressive stiffness as low as 0.70 MPa, can sustain physiologic compressive tractions on the order of 12 MPa with no apparent damage, due to the contribution of interstitial fluid pressure.

The aggregate modulus and permeability measured in the current study are in the range of values reported previously for bovine articular cartilage.^{4,5,11,21,24,27,33} The relatively low value of the permeability constant is due to the elevated tare loads employed in this study, which produced a tare equilibrium tissue strain of approximately 20% before sinusoidal loading was applied.

The theoretical analysis performed in this study was based on the tare configuration; thus, the specimen thickness h employed in the analysis corresponded to the tissue dimension after tare loading. The use of an infinitesimal strain biphasic analysis was justified because, relative to the tare configuration, the sinusoidal load produced tensile or compressive strains of 5% (at the interface with the porous filter) or less.

As noted earlier, for each of the two batches of nine specimens, the material properties were obtained by curve-fitting the time-dependent surface displacement response at only one of the tested frequencies for each sample (0.0001 Hz for group I and 0.0005 Hz for group II). The theoretical pressure response (at all frequencies) and the theoretical displacement response (at all frequencies other than that used for curvefitting) were predicted from the governing biphasic equations using the aggregate modulus²⁷ and permeability determined from the curvefit at the lowest frequency. This approach served to validate the biphasic model in confined compression by demonstrating good theoretical predictions of multiple experimental measurements on the same sample. The reason for using the lowest, rather than any other of the tested frequencies, for curvefitting is that this frequency was closest to the characteristic frequency f_c of the tissue. As discussed above, there exists substantial interstitial fluid flow throughout the depth of cartilage near this frequency,^{11,18} and this fluid flow is governed in part by the tissue permeability. At higher testing frequencies, the most substantial fluid flow is restricted to a narrow boundary layer near the porous filter, while at lower frequencies, the fluid flow is negligible. Thus, the frequencies used for the curvefitting procedure were selected to yield a most representative value for the tissue permeability through the depth. Note that curvefitting the experimental time-dependent displacement data at one loading frequency in the time domain, as performed in the current study, is a slightly different approach from curvefitting the displacement amplitude and phase over all values in the frequency domain^{11,21} (see the Appendix). In the current study, by fitting in the time domain, the material constants extracted from the curvefit were validated on the same sample by predicting the time-dependent response at other loading frequencies.

As reported in our previous study,³³ measurements of interstitial fluid pressure in cartilage can be performed successfully as long as certain precautions are observed. One of the most important aspects of these measurements is to avoid the formation of air bubbles inside the transducer since the compliance of these bubbles would inevitably cause a nearly complete loss of signal measurement. Because of the small dimensions of the fluid chamber in the solid-state microchip transducer employed in this study (a cylindrical hole 1 mm in diameter and 1 mm deep, with the piezoresistive sensing element

coated on the bottom and in contact with fluid only), it was relatively straightforward to avoid air bubbles by filling this chamber slowly using a syringe. Nevertheless, the actual measurements of pressure were relied upon to determine whether air bubbles had formed while filling the test chamber with bathing solution; thus, in order to make this determination early in the testing protocol, all specimens were tested starting with the highest loading frequency. This prevented randomizing the order of loading frequencies which may otherwise have been appropriate in light of the long testing duration and potential degradation of the tissue mechanical properties. However, it was encouraging to find that the material properties obtained by curvefitting the last (lowest frequency) test could properly predict the tissue response for all earlier (higher frequency) tests, thereby alleviating these concerns.

For this study the fastest frequency allowable for the testing device was 0.1 Hz since, under load control at higher frequencies, the displacement would approach submicron values [Fig. 3(a)] that fall below the step size of the device's stepper micrometer displacement actuator. The influence of the displacement step size on the correlation between the experimental and theoretical displacement can be observed in the decreasing value of the displacement r^2 with increasing frequency in Table 1, which can be attributed to the corresponding decrease in "signal-to-noise" ratio (no such signal degradation occurs with the pressure transducer with increasing frequency). Despite this limitation, there is no indication in the observed experimental trends that the behavior of the tissue would be any different than that predicted by theory at higher frequencies (Fig. 3). In the present study, apparatus compliance was measured prior to testing of the cartilage samples, and subtracted from the raw displacement measurements prior to performing the theoretical analysis. Therefore, the experimental and theoretical results of Figs. 3(a) and 3(b) appear qualitatively different from equivalent results in the study of Frank and Grodzinsky¹¹ who presented both analytical and experimental results that incorporate system compliance.

In this study it is found experimentally that interstitial fluid pressurization develops at frequencies as low as 10^{-4} Hz [Fig. 3(c)]; thus, even a loading cycle which takes 2.8 h (10^4 s) to complete results in significant interstitial fluid pressurization. It is reasonable to extrapolate these results to physiological conditions in human diarthrodial joints by noting that all activities of daily living involve some amount of motion and deformation, at frequencies in excess of 10^{-4} Hz, even in seemingly static postures such as standing and sitting; the implication of the experimental findings of this study is that a state of interstitial fluid pressurization is likely to occur at all times within normal articular cartilage, which may have important implications in our understanding of car-

tilage metabolism and chondrocyte biology under physiological conditions. This study complements previous reports of interstitial fluid pressure measurements in confined compression creep and stress-relaxation.^{28,33} Together, these studies strongly support the hypothesis that fluid pressurization occurs under virtually all loading regimes of articular cartilage and that interstitial fluid pressure effectively does not subside under loading. The agreement between theory and experiment reported in this study also provides support for theoretical analyses of articular contact^{1,2,19,22} and experimental measurements of cartilage friction^{3,25} which similarly refer to the importance of interstitial fluid pressurization in the load support mechanism of articular cartilage. These findings increase our understanding of cartilage mechanics and clarify the relative contribution of hydrostatic fluid pressure and solid matrix deformation in the load environment of chondrocytes as a function of loading frequency; they may also help elucidate the pathomechanics of osteoarthritis if it can be established that loss of interstitial fluid pressurization and the concomitant increase in tissue strain adversely affect chondrocyte metabolism by upsetting the delicate balance between normal tissue degradation and repair. The methodology presented here can be used in future studies to similarly analyze the relative magnitude of interstitial fluid pressurization in degenerative tissue.⁷

ACKNOWLEDGMENT

This study was supported by a grant from the National Institutes of Health (1R29-AR43628).

APPENDIX

The steady-state response of a biphasic cartilage plug in confined compression under the action of a static offset load superposed with a sinusoidal load can be derived by taking the limit of Eq. (4) as $t \rightarrow \infty$, whereby the exponential terms reduce to zero. Alternatively, this solution can be achieved using the method of complex variables, e.g., as presented by Lee *et al.*²¹ to yield

$$\frac{\bar{u}(z,f)}{h} = -\frac{P_0 z}{H_A h} - \frac{P_A}{\beta H_A} \frac{\sinh \beta(z/h)}{\cosh \beta}, \quad (\text{A1})$$

$$\bar{p}(z,f) = P_A \left(1 - \frac{\cosh \beta(z/h)}{\cosh \beta} \right),$$

where $\beta = \sqrt{i2\pi fh^2/H_A k_0}$, $i^2 = -1$, with the amplitude and phase of the frequency-dependent complex displacement, $\bar{u}(z,f)$, providing the desired solution. The equivalence of this solution with the limit of steady-state response in Eq. (4) has been verified numerically. For

the case of a linear isotropic biphasic poroviscoelastic material described by Mak,²³ a solution can be obtained by the same complex variables method^{23,32} which has the form of Eq. (A1) with

$$\beta = \left[\frac{i2\pi fh^2}{H_A k_0 \left(1 + c \ln \frac{1 + i2\pi f \tau_2}{1 + i2\pi f \tau_1} \right)} \right]^{1/2}, \quad (\text{A2})$$

where c , τ_1 , and τ_2 are three additional material constants describing the intrinsic viscoelasticity of the solid matrix. It can be verified that, when $c=0$ or $\tau_1 = \tau_2$, the solution reduces to the case of a linear isotropic biphasic material.

REFERENCES

- ¹ Ateshian, G. A. A theoretical formulation for boundary friction in articular cartilage. *J. Biomech. Eng.* 119:81–86, 1997.
- ² Ateshian, G. A., and H. Wang. A theoretical solution for the frictionless rolling contact of cylindrical biphasic articular cartilage layers. *J. Biomech.* 28:1341–1355, 1995.
- ³ Ateshian, G. A., H. Wang, and W. M. Lai. The role of interstitial fluid pressurization and surface porosities on the boundary friction of articular cartilage. *J. Tribol.* 120:241–251, 1998.
- ⁴ Ateshian, G. A., W. H. Warden, J. J. Kim, R. P. Grelsamer, and V. C. Mow. Biphasic finite deformation material properties of bovine articular cartilage from confined compression experiments. *J. Biomech.* 30:1157–1164, 1997.
- ⁵ Athanasiou, K. A., M. P. Rosenwasser, J. A. Buckwalter, T. I. Malinin, and V. C. Mow. Interspecies comparison of *in situ* intrinsic mechanical properties of distal femoral cartilage. *J. Orthop. Res.* 9:330–340, 1991.
- ⁶ Bachrach, N. M., V. C. Mow, and F. Guilak. Incompressibility of the solid matrix of articular cartilage under high hydrostatic pressures. *J. Biomech.* 31:445–451, 1998.
- ⁷ Broom, N. D., and A. Oloyede. The importance of physicochemical swelling in cartilage illustrated with a model hydrogel system. *Biomaterials* 19:1179–1188, 1998.
- ⁸ Buschmann, M. D. Numerical conversion of transient to harmonic response functions for linear viscoelastic materials. *J. Biomech.* 30:197–202, 1996.
- ⁹ Buschmann, M. D., Y. A. Gluzband, A. J. Grodzinsky, J. H. Kimura, and E. B. Hunziker. Chondrocytes in agarose culture synthesize a mechanically functional extracellular matrix. *J. Orthop. Res.* 10:745–758, 1992.
- ¹⁰ Buschmann, M. D., J. Soulhat, A. Shirazi-Adl, J. S. Jurvelin, and E. B. Hunziker. Confined compression of articular cartilage: Linearity in ramp and sinusoidal tests and the importance of interdigitation and incomplete confinement. *J. Biomech.* 31:171–178, 1998.
- ¹¹ Frank, E. H., and A. J. Grodzinsky. Cartilage electromechanics. II. A continuum model of cartilage electrokinetics and correlation with experiments. *J. Biomech.* 20:629–639, 1987.
- ¹² Fung, Y. C. B. Quasi-linear viscoelasticity of soft tissues. In: *Biomechanics: Mechanical Properties of Living Tissues*, New York: Springer, 181, pp. 226–237.
- ¹³ Gray, M. L., A. M. Pizzanelli, A. J. Grodzinsky, and R. C. Lee. Mechanical and physicochemical determinants of the

- chondrocyte biosynthetic response. *J. Orthop. Res.* 6:777–792, 1988.
- ¹⁴ Guilak, F., B. A. Best, A. Ratcliffe, and V. C. Mow. Instrumentation for load and displacement controlled studies on soft connective tissues. *Biomech. Symp.*, ASME, AMD 98:113–116, 1989.
- ¹⁵ Guilak, F., B. C. Meyer, A. Ratcliffe, and V. C. Mow. The effects of matrix compression on proteoglycan metabolism in articular cartilage explants. *Osteoarthritis Cartilage* 2(2):91–101, 1994.
- ¹⁶ Guilak, F., R. L. Spilker, J. K. Suh, and V. C. Mow. A biphasic finite element model of the mechanical response of articular cartilage to cyclic compression. *J. Biomech. Eng.* in press.
- ¹⁷ Higginson, G. R., and J. E. Snaith. The mechanical stiffness of articular cartilage in confined oscillating compression. *IMEchE*. 8:11–14, 1979.
- ¹⁸ Holmes, M. H., W. M. Lai, and V. C. Mow. Singular perturbation analysis of the nonlinear, flow-dependent compressive stress relaxation behavior of articular cartilage. *J. Biomed. Eng.* 107:206–218, 1985.
- ¹⁹ Kelkar, R., and G. A. Ateshian. Contact creep of biphasic cartilage layers: Identical layers. *J. Appl. Mech.* 66:137–145, 1999.
- ²⁰ Kvalseth, T. O. Cautionary note about R^2 . *Am. Stat.* 39:279–285, 1985.
- ²¹ Lee, R. C., E. H. Frank, A. J. Grodzinsky, and D. K. Roylance. Oscillatory compressional behavior of articular cartilage and its associated electromechanical properties. *J. Biomech. Eng.* 103:280–292, 1981.
- ²² Macirowski, T., S. Tepic, and R. W. Mann. Cartilage stresses in the human hip joint. *J. Biomed. Eng.* 116:11–18, 1994.
- ²³ Mak, A. F. Apparent viscoelastic behavior of articular cartilage—The contributions from the intrinsic matrix viscoelasticity. *J. Biomech. Eng.* 108:123–130, 1986.
- ²⁴ Mansour, J. M., and T. Matsumoto. Permeability of articular cartilage from small joints. *Trans. Annu. Meet. - Orthop. Res. Soc.* 23:479, 1998.
- ²⁵ McCutchen, C. W. The frictional properties of animal joints. *Wear* 5:1–17, 1962.
- ²⁶ Mow, V. C., J. S. Hou, J. M. Owens, and A. Ratcliffe. Biphasic and quasilinear viscoelastic theories for hydrated soft tissue. In: *Biomechanics of Diarthrodial Joints*, edited by V. C. Mow, A. Ratcliffe, and S. L.-Y. Woo. New York: Springer, 1990, Vol. II, pp. 215–260.
- ²⁷ Mow, V. C., S. Kuei, W. M. Lai, and C. G. Armstrong. Biphasic creep and stress relaxation of articular cartilage in compression: theory and experiments. *J. Biomed. Eng.* 102:73–84, 1980.
- ²⁸ Oloyede, A., and N. D. Broom. Is classical consolidation theory applicable to articular cartilage deformation? *Clin. Biomech.* 6:206–212, 1991.
- ²⁹ Parkkinen, J. J., M. J. Lammi, H. J. Helminen, and M. Tammi. Local stimulation of proteoglycan synthesis in articular cartilage explants by dynamic compression in vitro. *J. Orthop. Res.* 10:610–620, 1992.
- ³⁰ Sah, R. L. Y., Y.-J. Kim, J.-Y. H. Doong, A. J. Grodzinsky, A. H. K. Plaas, and J. D. Sandy. Biosynthetic response of cartilage explants to dynamic compression. *J. Orthop. Res.* 7:619–636, 1989.
- ³¹ Schinagl, R. M., M. K. Ting, J. H. Price, and R. L. Sah. Video microscopy to quantitate the inhomogeneous equilibrium strain within articular cartilage during confined compression. *Ann. Biomed. Eng.* 24:500–512, 1996.
- ³² Setton, L. A., W. Zhu, and V. C. Mow. The biphasic poroviscoelastic behavior of articular cartilage: Role of the surface zone in governing the compressive behavior. *J. Biomech.* 26:581–592, 1993.
- ³³ Soltz, M. A., and G. A. Ateshian. Experimental verification and theoretical prediction of cartilage interstitial fluid pressurization at an impermeable contact interface in confined compression. *J. Biomech.* 31:927–934, 1998.
- ³⁴ Suh, J. K. Dynamic unconfined compression of articular cartilage under cyclic compressive load. *Biorheology* 33:289–304, 1996.
- ³⁵ Suh, J. K., Z. Li, and S. L.-Y. Woo. Dynamic behavior of biphasic cartilage model under cyclic compressive loading. *J. Biomech.* 28:357–364, 1995.
- ³⁶ Torzilli, P. A., R. Grigieni, C. Huang, S. M. Friedman, S. B. Doty, A. L. Boskey, and G. Lust. Characterization of cartilage metabolic response to static and dynamic stress using a mechanical explant test system. *J. Biomech.* 30:1–9, 1997.
- ³⁷ Wayne, J. S. Load partitioning influences the mechanical response of articular cartilage. *Ann. Biomed. Eng.* 23(1):40–47, 1995.